THE ASTROPHYSICAL JOURNAL, **262**:497–510, 1982 November 15

A THERMAL WIND MODEL FOR THE BROAD EMISSION LINE REGION OF QUASARS

R. J. WEYMANN, J. S. SCOTT, AND A. V. R. SCHIANO
Steward Observatory, University of Arizona

AND

WAYNE A. CHRISTIANSEN
Department of Physics and Astronomy, University of North Carolina
Received 1982 January 6; accepted 1982 May 17

ABSTRACT

Arguments are summarized for supposing that the clouds giving rise to the broad emission lines of QSOs are confined by the pressure of an expanding thermal gas and that a flux of relativistic particles with luminosity comparable to the photon luminosity streams through this gas. The resulting heating and momentum deposition produces a transonic thermal wind whose dynamical properties are calculated in detail. This wind accelerates and confines the emission line clouds, thereby producing the broad emission line (BEL) profiles. In a companion paper, the properties of the wind at much larger distances ($\backsim$kpc) than the BEL region are used to explain the production of the broad absorption lines (BAL) observed in some QSOs. The same set of wind parameters can account for the properties of both the BEL and BAL regions, and this unification in the physical description of the BEL and BAL regions is one of the most important advantages of this model.

A characteristic size of $\backsim$1 pc for the QSO emission line region is one consequence of the model. This characteristic size is shown to depend upon luminosity in such a way that the ionization parameter is roughly constant over a wide range of luminosities. An X-ray luminosity due to thermal bremsstrahlung of $\sim$1%–10% of the optical luminosity is another consequence of the model. The trajectories of clouds under the combined influence of ram pressure acceleration and radiative acceleration are calculated. From these trajectories emission line profiles are also calculated, as well as the wind and cloud parameters yielding profiles in fair agreement with observed profiles explored. Opacity in the wind due to electron scattering displaces the line cores of optically thin lines to the blue. This is roughly compensated for by the redward skewing of optically thick lines due to preferential emission of photons from the back side of the clouds. Circumstances under which the relativistic particles can avoid rapid depletion due to Compton losses are discussed.

Subject heading: quasars

I. INTRODUCTION

In this paper we explore the effects of the existence of a very hot thermal wind on the broad emission line region (BELR) of quasars. In a companion paper (Scott *et al.* 1982, hereafter Paper II) we demonstrate that this same wind can also account for properties of the broad *absorption* features observed in the spectra of some QSOs. Indeed, it was the latter problem which initially motivated the work reported in the present paper.

Twenty years after their discovery, there is no general consensus concerning the dynamics or even kinematics of the BELR in QSOs. The following summary of the BELR properties, which we use in our model, probably represents a broad consensus, however.

Fairly satisfactory fits to the relative intensities of the lines can be obtained by assuming photoionization by a central small source with a power-law continuum (e.g., Kwan and Krolik 1981). The most satisfactory models require a large number of clouds which are individually optically thick in the Lyman continuum and have densities of order 10^9–10^{10} cm^{-3}. Those densities, coupled with the observed level of ionization, suggest typical distances for the material on the order of 1 pc from the center of the continuum source. The emitted flux in the emission lines, together with the density estimates and the distance estimate cited above, implies an exceedingly small filling factor for the ionized gas. The current consensus is that the well-known "Lyα/Hβ discrepancy" is most satisfactorily explained by "extra" creation of Balmer photons via collisions in an optically thick cloud rather than preferential destruction of Lyα. In this case, it is legitimate to use the Lyα equivalent width to estimate the covering factor of the clouds, which is of order 5%–10% (see Baldwin and Netzer 1978; Smith *et al.* 1981). In principle, this covering factor could arise in situations ranging from a relatively small number of large clouds, any one of which completely covers the continuum source, to a very large number of small clouds, none of which individually covers the source. We will assume the latter limit is nearer the truth on the basis of reasons discussed by Carswell and Ferland (1980), although Capriotti, Foltz, and Byard (1981) present arguments in the case of lower luminosity objects (e.g., Seyfert galaxies) why the other extreme may be more appropriate. There are no secure estimates concerning the sizes of the BELR clouds for high luminosity QSOs. Time scales for polarization changes in some OVV objects as short as several hours (Angel and Stockman, 1980) suggest that the continuum-producing region in these objects may be $\sim 10^{15}$ cm, implying that the BELR clouds are $\ll 10^{15}$ cm, but the optical continuum-producing region in the more quiescent QSOs may be substantially larger. The relative intensities of the emission lines (e.g., C IV, Mg II, Lyα, and Hβ) are most readily interpreted with column densities $10^{22}-10^{23}$ cm^{-2}, implying cloud thicknesses $\sim 10^{13}$ cm for densities of 3×10^9. Clouds much thicker than this would produce C II $\lambda 2326$ emission in excess of that observed (Kwan and Krolik 1981). We adopt 2×10^{25} g as a typical cloud mass.

At a speed $v \approx 10^4$ km s^{-1}, the time for clouds to move a distance comparable to the size of the BELR region is then 3×10^9 s^{-1}. At an internal temperature of $T = 20{,}000$ K the adiabatic sound speed is ≈ 25 km s^{-1}. Thus, a cloud created with a characteristic size of 10^{13} cm doubles its size in a time of order 10^{-3} of the crossing time, if allowed to expand freely. Numerous authors have therefore assumed that the clouds must be confined. We agree, but believe the arguments are somewhat more subtle than generally stated. In particular, we know of no convincing spectroscopic argument why the clouds must be confined. However, Krolik, McKee, and Tarter (1981) have shown that the thermal properties of the material are such that an unconfined cloud will be rapidly heated to the point where the pressure from the hot debris of such clouds which have expanded will stop further expansion. We assume in what follows, therefore, that the clouds are confined by gas pressure and/or ram pressure.

Most discussions of the dynamics and kinematics of the BELR based upon analysis of the line profiles have concluded that the motions are predominantly radial rather than rotational and probably involve expansion rather than infall (Capriotti, Foltz, and Byard 1980), although Smith *et al.* (1981) and Wilkes and Carswell (1981) argue that radial expansion is in conflict with the absence of strong red asymmetry in the Lyα profiles. Shields (1978) has reviewed the various arguments concerning outflow versus rotation. We think these arguments favor radial expansion, but concede they are not compelling. We present additional theoretical arguments below, strongly implying radial expansion. We will return to the question of the line profiles in § IV where we will see that effects associated with our model somewhat mitigate the red asymmetry.

Mathews (1981) and Blumenthal and Mathews (1975, 1979) developed a dynamical model for the BELR involving radiative acceleration of optically thin clouds. These models were very attractive because they predicted a logarithmic profile in the wings which is in reasonable accord with the observations, with little dependence upon specific parameters. They invoked a very hot, possibly relativistic medium to confine the clouds. This medium did not play a crucial role in their dynamical picture, although the drag produced on the clouds moving through this medium was considered. However, if an extremely hot medium surrounds the central source, then its dynamical effects are likely to be at least as important as the radiation itself in accelerating the clouds.

II. RATIONALE FOR A THERMAL WIND

That hot thermal winds are, in fact, a general feature of QSOs seems to us almost inevitable. The argument of Krolik, McKee, and Tarter (1981) implies the existence of a confining gas, which even in the absence of heating mechanisms other than Compton heating will reach temperatures $\sim 10^8$ K. Unless there is a central mass $\gtrsim 10^9\ M_\odot$ present, this gas must stream out in a wind. However, for the following reasons we believe it likely that an additional heat source exists, namely, a flux of relativistic particles:

1. If the gas were as cool as $\sim 10^8$ K, its expansion speed would be rather low, and the drag on clouds in pressure equilibrium with such a medium would be so great that radiative acceleration could not produce much additional velocity: at ~ 1 pc, a luminosity of 10^{46} ergs s^{-1} drives the clouds to a differential velocity of only ~ 400 km s^{-1} for a wind density of 10^6 cm^{-3}. The low wind velocity and small differential velocity between cloud and wind yield line profiles which are too narrow to fit typical observed profiles. The same considerations apply to models with clouds confined by a static medium whose dynamics are dominated by gravity and which are moving in bound orbits or undergoing radial infall. At a distance of 1 pc and a central mass of $10^9\ M_\odot$ the drag associated with a medium having $n \approx 10^6$ cm^{-3} limits the velocity of the clouds to ~ 250 km s^{-1}. The medium must therefore be substantially hotter than 10^8 K, implying outflow.

2. The existence of γ-ray emission in 3C 273 (Bignami *et al.* 1981) almost certainly demands the presence of relativistic electrons in this QSO, although until the sensitivity of the γ-ray measurements are improved, we cannot say whether a strong γ-ray flux is as widespread a feature in QSOs as is X-ray emission.

3. Models of the compact spherically symmetric ("halo") VLBI components seen in some radio sources require the presence of relativistic electrons with energies ~ 500 Mev on scales of a few parsecs or less. The densities of such particles are such that if they are radially streaming, they represent an energy output comparable to the photon luminosity (Jones 1979; Jones and Hardee 1979). The question remains open as to whether such particles are associated only with strong radio sources or are a general feature of all QSOs. As discussed in § V, it may simply be that QSOs with compact radio halos differ from radio-quiet QSOs only in that the radio emitters happen to have relatively large magnetic fields entrained in the wind.

4. It has often been suggested that an underlying nonthermal power law is a universal feature of the IR, optical, and UV spectra of all QSOs. Such a power-law spectrum would most likely originate from synchrotron radiation, and this strongly suggests that relativistic particles are present in all QSOs.

As a consequence of these considerations, the fundamental assumption is made in this paper that a stream of relativistic particles with γ's of order 1000 and total luminosity comparable to the photon luminosity is a general attribute of all QSOs and that such particles exist throughout most of the BELR. Such particles inevitably provide a strong heat source to the thermal gas as discussed below. (In § V we discuss the survival of these particles against Compton losses.)

As demonstrated in § III, this thermal wind model leads naturally to the characteristic size of the BELR. In order to accelerate the massive clouds producing the broad absorption lines (as discussed in Paper II), a large momentum flux is required, and in this respect the nonrelativistic thermal wind has the advantage of being energy efficient: for a given expenditure of energy more momentum is available for cloud acceleration when the energy is converted from relativistic particles to expansion of a subrelativistic wind.

We further assume that on the scales we are dealing with ($\gtrsim 10^{17}$ cm), the wind can be considered spherically symmetric and in a steady state. We now consider in some detail the properties of such a wind.

III. PHYSICAL PROPERTIES OF THE WIND

a) *Basic Equations and Assumptions*

The basic equations are just those for spherically symmetric, steady flow:

$$V\frac{dV}{dr} = -\frac{GM}{r^2} - \frac{1}{\rho}\frac{dP}{dr} + \frac{1}{\rho}\frac{\Phi}{c}, \tag{1}$$

$$\frac{1}{r^2}\frac{d}{dr}(\rho V r^2) = S_{\rm th}, \tag{2}$$

$$V\frac{d}{dr}\left(\frac{3}{2}\frac{P}{\rho}\right) = \frac{PV}{\rho^2}\frac{d\rho}{dr} + \frac{\Phi}{\rho}\left(1 - \frac{v}{c}\right) - \frac{\psi}{\rho}, \tag{3}$$

$$P = \frac{2\rho kT}{m_{\rm H}}, \tag{4}$$

The quantity $\Phi(r)$ represents the rate at which the relativistic electrons lose energy to the thermal gas; $\Phi(r)/c$ in equation (1) is the corresponding momentum deposition rate. In equation (3) the fraction $(1 - V/c)$ is the portion of the energy loss going toward increasing the thermal energy of the gas; the remainder appears as increased bulk kinetic energy. The quantity ψ is the radiation loss suffered by the gas (ergs cm^{-3} s^{-1}).

Krolik, McKee, and Tarter (1981) considered a variety of heat sources which could raise the temperature of the gas over the Compton interaction value of $\sim 10^8$ K. In particular, they considered Coulomb heating by suprathermal particles. However, as discussed recently by Scott *et al.* (1980), complex collective effects in the plasma involving the oscillating two-stream instability (OTS) yield heating rates from relativistic electrons orders of magnitude larger than those associated with simple binary Coulomb interactions. The expression given for the heating rate by Scott *et al.* (1980) may be written

$$\Phi = 1.6 \times 10^{-4} \frac{n_{\rm rel}^3}{n_{\rm th}^{3/2}} \frac{1}{\gamma_{\rm min}} \text{ ergs cm}^{-3}\text{ s}^{-1}, \tag{5}$$

where $n_{\rm rel}$ is the relativistic particle density, $\gamma_{\rm min}$ the minimum γ of the relativistic particles, and $n_{\rm th}$ is the density of the thermal gas. If we assume radially streaming relativistic particles, then we may rewrite equation (5) as

$$\Phi = 5.5 \times 10^{-21} L_{\rm rel}^3 / \left(r^6 \gamma_{\rm min}^4 n_{\rm th}^{3/2}\right), \tag{6}$$

where $L_{\rm rel}$ is the relativistic particle luminosity.

Equations (1)–(4) and (6) must then be supplemented by

$$\frac{dL_{\rm rel}}{dr} = -4\pi r^2 \left(\Phi - m_e c^2 \gamma S_{\rm rel}\right). \tag{7}$$

Besides the OTS heating mechanism, the relativistic particles suffer other losses; in particular, the particles will give up energy to the radiation field via inverse Compton scattering. We have not included Compton losses in the numerical calculations described below, but we shall consider them later in the discussion of § V.

Krolik *et al.* also thoroughly explored the various processes likely to be most important in cooling the thermal gas. In the cooler, denser regions of our flows, free-free radiation and the Compton interaction are dominant and comparable in importance, but we have only included free-free radiation. (In fact, in the outer regions of the flow, Compton cooling dominates over free-free cooling, but the heating and expansion dominate the thermodynamics of the gas in the strongly expanding portion of the flow, so its neglect is not crucial. In subsequent treatments however, Compton cooling should be included.)

The source terms $S_{\rm th}$ and $S_{\rm rel}$ in equations (2) and (7) represent the rate at which thermal gas and relativistic particles are injected into the flow, the former by, for example, stripping of stars near the central source (Edwards 1980), boiloff of gas from an inner disk (Shields 1977), or disruption of the cool line-emitting clouds themselves. We speculate that the relativistic particles may enter the flow by diffusion away from jets or would-be jets where they are generated.

Our understanding of either the production of thermal gas or relativistic particles is still so poor, however, that it does not seem worthwhile to attempt to model the spatial injection functions. Therefore, we shall simply assume that the thermal gas and relativistic particles have been deposited within some minimum distance $r_{\rm min}$ (i.e., $S_{\rm th}=S_{\rm rel}=0$ for $r>r_{\rm min}$) and consider the flow only for $r>r_{\rm min}$. A further simplification involves neglecting the evolution of the energy spectrum of the electrons by simply assuming they are monochromatic, so that $\gamma \equiv \gamma_{\rm min}$.

With these assumptions, we now examine the properties of the flow. We suppose the gas to be injected with zero or very small net outward radial velocity so that the flow is initially subsonic. Since the wind must accelerate both emission line region clouds and the more distant and larger absorption-producing clouds to very high velocities, we are interested in the transonic solution to the flow equations yielding very high terminal velocities. Equations (1)–(4) yield two differential equations for V and T:

$$\frac{d\ln V}{d\ln r}=\frac{r}{PV}\left[\frac{2}{5}(\Phi-\psi)-\frac{V}{c}\Phi + \frac{3}{5}\frac{GM\rho V}{r^2}\Big/(1-V^2/W^2)\right]-2, \quad (8)$$

$$\frac{d\ln T}{d\ln r}=-\frac{2}{3}\frac{d\ln V}{d\ln r}-\frac{4}{3}+\frac{2}{3}\frac{r}{PV}\left[\Phi\left(1-\frac{V}{c}\right)-\psi\right], \quad (9)$$

where $W=(5p/3\rho)^{1/2}$ is the adiabatic sound speed. The transonic ("critical") point is found by setting the numerator and denominator of equation (8) simultaneously to zero. The transonic condition then implies a relation of the form $r_{\rm sonic}=r(P,T,L_{\rm rel},M)$. Specifying these four variables at the sonic point specifies uniquely the transonic radius. The transonic solution is started by expanding equations (8) and (9) about the sonic point and then numerically integrating equations (7), (8), and (9) inward to whatever $r_{\rm min}$ we choose (within which thermal and relativistic particle injection becomes important) and outward, to the point where the flow has essentially reached its terminal velocity.

For the range of parameters of most interest (see below) the cooling and gravitational terms are not important, and, with $V/c \ll 1$, we have approximately $r_{\rm sonic} \approx (5pV/\Phi)$, i.e., the transonic point occurs where the characteristic flow time approximates the heating time. Numerically, using equation (6), we find

$$r_{\rm sonic}\approx\left[\frac{L_{46}^{3/5}T_{10}^{1/5}}{\gamma_3^{4/5}P_{-2}^{1/2}}\right]\ {\rm pc}, \quad (10)$$

where L_{46} is the relativistic electron luminosity at the sonic point in units of 10^{46} ergs s^{-1}, γ is the γ of the electrons in units of 10^3, and P_{-2} the wind pressure in units of 10^{-2} dynes cm^{-2}, all evaluated at the sonic point.

There are several remarks to be made concerning equation (10). (i) The sonic point marks the point where the flow, and hence the clouds, is being strongly accelerated so that the number density of embedded clouds (assuming they obey the equation of continuity) drops rapidly beyond this point. Thus, $r_{\rm sonic}$ is a measure of the characteristic size of the emission line region, and it is an encouraging feature of the model that $r_{\rm sonic}$ is about the same size as the BELR deduced on the basis of the observed ionization state of the clouds (see § I). (ii) The value of $r_{\rm sonic}$ depends more on the *number* of relativistic particles being emitted rather than on the total luminosity of such particles. (iii) Since the pressure in the wind at the sonic point is of the same order as the pressure in the emission line region clouds ($P\approx 2nkT\approx 2\times3\times10^9 \times1.38\times10^{-16}\times2\times10^4=1.7\times10^{-2}$ dynes cm^{-2}), we may regard the pressure as fixed empirically. Thus, $r_{\rm sonic}$ is very insensitive to the temperature of the sonic point. (iv) It has long been noted that the ionization parameter $n_{\rm photon}/n_{\rm electron}$ varies by a surprisingly small amount between the Seyfert nuclei and QSOs despite a range of $\sim10^4$ in the luminosity of these objects (Shields 1978). Since the densities in the BELR regions of Seyfert galaxies and QSOs appear to be comparable, models to explain this phenomenon require that the predicted size of the BELR scale with luminosity approximately so as to keep the ionizing flux nearly constant. In our model the characteristic size of the BELR is set by the sonic point radius, since it is here that the wind is accelerated to high velocities. If we use equation (10) for the sonic point, assume pressure balance between the cloud and hot medium, and suppose that the number flux and energy flux of the particles are proportional to the photon flux, then the ionization parameter implied by our model scales as

$$\frac{n_{\rm phot}}{n_{\rm elect}} \approx \frac{T_{\rm cloud}}{L_{\rm rel}^{1/5} T_{\rm wind}^{2/5}} . \quad (11)$$

The temperature of the clouds is tightly regulated by cooling from emission lines and will therefore be relatively constant. We cannot predict *a priori* the variation of the wind temperature from Seyfert galaxies to QSOs, but the wind temperature is closely related to the line widths which are observed to be nearly constant from Seyfert I galaxies through high luminosity QSOs. Equation (11) then suggests only a very weak dependence in the ionization parameter upon luminosity, as required by the observations.

b) *Choice of Parameters for Numerical Solutions*

We have carried out numerical solutions of equations (1)–(4) and (7) for a variety of wind parameters in order to gain some feeling for the dependence of the wind characteristics on these parameters. In all cases the pressure at the sonic point was fixed so that $(nT)_{\rm wind} = 10^{14}$, following the discussion above concerning the pressure in the BELR clouds.

In accordance with our assumption that $L_{\rm rel} \approx L_{\rm photon}$, $L_{\rm rel}$ is taken of order 10^{46}. Following the discussion in § II, we have considered γ to be ~ 1000. This is quite reasonable, since, as discussed in § V, particles produced with γ much in excess of 1000 will rapidly lose their energy via Compton interactions. On the other hand, particles with $\gamma \ll 1000$ lose their energy very rapidly via the oscillating two-stream instability (eq. [6]). The mass of the putative condensed central object has been taken to be $\sim 10^8\ M_\odot$, the Eddington mass for a luminosity of 10^{46} ergs s^{-1}. Of course, there is no *a priori* reason why the central mass could not be substantially larger than this, and if it were as large as, say $\sim 10^{10}\ M_\odot$, then even very hot gas would be confined, and infall velocities for the clouds comparable to those observed in the BELR would result. Our basic thesis, however, is that the same mechanism which produces broad *absorption* line clouds (which clearly *are* moving outward) can also account for the BELR properties. Therefore, we have not investigated the consequences of such large central masses. The wind temperature is not likely to rise in excess of 10^{10} K because the heating mechanism drops rapidly in efficiency as the electrons become relativistic. For the nominal values of the other parameters indicated above, it was found that transonic solutions do not exist for $T < 10^8$. Therefore, we have varied T about a nominal value of 10^9 K.

c) *Results of Numerical Integrations*

The results of the numerical integrations of the wind equations are summarized in Table 1 and Figure 1. The solution incorporating the nominal values of the parameters described above is given as solution 1. Each of the parameters characterizing the flow has then been varied independently (except the sonic point density) over a factor of 10 about these nominal values (solutions 2–9). (The choice of parameters for solution 10 is explained in § IV.) The first five rows give the parameters characterizing the solutions. The remaining rows (6–12) give, respectively, the sonic point radius, the inner radius, $r_{\rm min}$, the log of the particle luminosity at the inner radius, the total free-free luminosity emitted beyond $r_{\rm min}$, the mass loss rate, the flow of kinetic energy through a sphere with radius very large compared to the sonic point radius, and the terminal velocity of the flow. Figure 1 shows the variation with radius of the velocity, temperature, and density of the wind for solution 1.

All of the cases we have investigated which have solutions which pass from subsonic to supersonic at the critical point (this includes all the solutions in Table 1)

TABLE 1

PROPERTIES OF BROAD EMISSION LINE REGION WIND SOLUTIONS

Quantity	Solution 1	2	3	4	5	6	7	8	9	10
$\log T_{\rm sonic}$	9.0	9.5	8.5	9.0	9.0	9.0	9.0	9.0	9.0	9.35
$\log n_{\rm sonic}$	5.0	4.5	5.5	5.0	5.0	5.0	5.0	5.0	5.0	4.65
$\log L_{\rm rel(sonic)}$	46.0	46.0	46.0	46.5	45.5	46.0	46.0	46.0	46.0	45.88
$\log \gamma$	3.0	3.0	3.0	3.0	3.0	2.5	3.5	3.0	3.0	2.81
$\log M/M_\odot$	8.0	8.0	8.0	8.0	8.0	8.0	8.0	8.5	7.5	8.0
$r_{\rm sonic}$ (pc)	0.38	0.48	0.31	0.76	0.19	0.96	0.15	0.39	0.38	0.53
$r_{\rm min}$ (pc)	0.03	0.03	0.03	[0.15]	0.3	[0.03]	0.03	0.03	[.07]	0.03
$\log L(r_{\rm min})$	46.05	46.11	46.03	46.55	45.53	46.72	46.01	46.05	46.04	46.05
$\log L_{\rm X\text{-}ray}$	44.57	44.68	44.56	44.90	43.43	46.57	42.8	44.66	44.13	45.00
$\dot{M}$ ($M_\odot$ yr^{-1})	24.6	21.5	27.9	97.1	6.2	153.5	3.9	25.0	24.4	31.8
$\log L({\rm KE}_\infty)$	45.91	46.02	45.83	46.42	45.40	46.13	45.80	45.91	45.91	46.00
V_∞(10^3 km s^{-1})	32.5	39.1	27.7	29.3	36.4	16.7	71.4	32.0	32.6	30.0

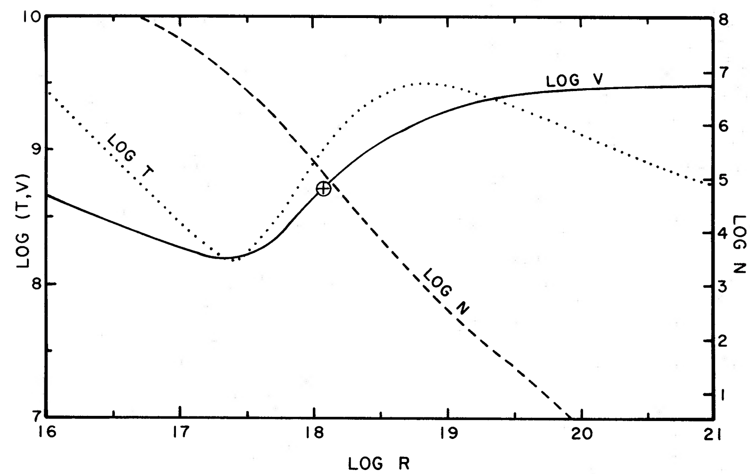

FIG. 1.—Run of wind velocity, temperature (*left scale*), and density (*right scale*) for solution 1. Circle marks the sonic point. Minimum in velocity and temperature occurs at the radius within which the heating and cooling terms approximately balance.

have qualitatively the same behavior as solution 1 beyond the critical point: the velocity rises monotonically to its terminal velocity, the temperature passes through a maximum somewhat beyond the critical point and then slowly falls. In the regime where the velocity has essentially reached its terminal value it can be shown that the particle luminosity goes slowly to zero, as $1/(\ln r)^{1/2}$. Even though two critical solutions passing through the sonic point may exist, it may be that neither pass from subsonic to supersonic: in particular, for sonic point temperatures below $T \approx 10^8$ both solutions go from supersonic to subsonic as the radius increases. Such solutions cannot be continued to large radii. Inspection of Table 1 shows that the properties of the solution at and beyond the sonic point are quite insensitive to the central mass and sonic point temperature, moderately sensitive to the particle luminosity, and quite sensitive to the γ of the particles.

The behavior of the solutions inside the sonic point is more complex. The temperature and velocity minimum at ~ 0.1 pc shown in Figure 1 for solution 1 is characteristic of most of the solutions and marks approximately the point inside which the free-free cooling closely balances the heating from the relativistic particles. Eventually at $r \approx 10^{-3}$ pc the velocity reaches a maximum, but the validity of the physical assumptions leading to these solutions surely breaks down at radii much larger than this. In the case of solution (6) ($\log \gamma = 2.5$), the velocity has a flat section and then drops precipitously at $r < 0.07$ pc. Between the sonic point and the temperature minimum the temperature drops so rapidly that the flows stay nearly sonic despite the decrease in velocity. Indeed, for two of the cases (4, 9), the solutions attempt to become supersonic again and become singular.

There are several possible observational consequences of the existence of a stream of relativistic particles and the associated thermal wind in QSOs. One is the character of the line profiles which would result from dense clouds accelerated by such flows. Others involve the question of the presence (or absence) of radio emission, X-ray emission from thermal bremsstrahlung, and damping of intrinsic variability due to electron scattering. We consider the first of these in § IV and consider the others more briefly in § V.

IV. CLOUD MOTIONS AND LINE PROFILES

a) Cloud Trajectories

The origin of the clouds making up the BELR is no better understood than the origin of the intercloud medium or, for that matter, the origin of the material feeding the accretion disk powering the QSO. Since we are assuming spherical outflow on scales comparable to the sonic point radius, the source of the matter must either be primordial (i.e., the QSO was born with a disk $\sim 10^7$–10^8 $M_\odot$ already in existence), or the matter must fall through the wind in a condensed form, probably as heavy clouds, as we discuss below.

In the following, we assume that a cool dense cloud suddenly appears at some point in the flow. If the cloud condenses from the hot medium via a thermal instability (see Eilek and Caroff 1979; Beltrametti 1981), then the initial cloud velocity is equal to the wind velocity. Although our winds are also thermally unstable on time scales short compared to the crossing time for regions inside the velocity minimum, the density contrast between the clouds and the wind is so large that unless the magnetic field energy density is initially many orders of magnitude smaller than the thermal energy in the wind, it would vastly exceed the thermal energy in the condensed cloud. Unless the geometry of the field is highly ordered, cloud formation would be inhibited.

On the other hand, if the clouds result from material ablated off stars (or infalling very heavy clouds) as they fall through the wind, the clouds will initially have the velocity of the star or heavy clouds. We believe this possibility is more likely than thermal instability for the reason just stated.

We consider the following equations of motion for an individual cloud:

$$\ddot{r}_{\rm cl}=\left[C_1\rho_w|V_w-V_{\rm cl}|(V_w-V_{\rm cl})+\frac{L_{\rm phot}f}{4\pi r^2 c}\right]\frac{\pi a^2}{M_{\rm cl}}-\frac{GM_{\rm bh}}{r_{\rm cl}^2}, \tag{12}$$

$$M_{\rm cl}=C_2\pi a^3\rho_{\rm cl}, \tag{13}$$

$$P_w+\rho_w(V_w-V_{\rm cl})^2=P_{\rm cl}\equiv\rho_{\rm cl}W_{\rm cl}^2, \tag{14}$$

In equation (12), the three terms on the right-hand side represent the effects of drag, radiative acceleration, and gravity for clouds with mass $M_{\rm cl}$ and cross section πa^2. A fraction f of the UV photons are absorbed within the cloud; the remainder pass through it. This fraction was estimated by solving in a very approximate way for the ionization structure within the cloud to yield its optical depth, assuming an incident power law with spectral index $-3/2$. The "constants" C_1 and C_2 in equations (12) and (13) are slowly varying functions of the Mach number which we set to unity. Equation (14) simply represents the conservation of momentum along the axis of the cloud. The thermal velocity within the cloud, $W_{\rm cl}$, is assumed fixed at a value corresponding to a temperature of 2×10^4 K.

The momentum transport associated with the relativistic particles (which is comparable to that associated with the photons) has not been included in equation (12). We have also neglected the contribution of the momentum flux of the relativistic particles and photons in confining the cloud (eq. [14]). We have thus ignored the many subtleties involving the influence of the radiation pressure on the shape of the cloud, discussed in detail by Blumenthal and Mathews (1979).

The essential features of equations (12)–(14) are that clouds with the properties described in § I ($M_{\rm cl}\approx2\times10^{25}$ g), when injected at ~0.1 pc into winds like those in Table 1, rapidly approach the speed of the wind over a distance small compared to other scales of the flow. Radiative acceleration initially drives the clouds faster than the wind speed, but drag always prevents the clouds from moving at a speed very much different from the wind speed. In Figure 2 we show, along with the wind velocity, the actual velocity of a cloud injected at rest at a distance of 0.1 pc. Also shown is the "critical cloud mass" as a function of distance from the center. Clouds above the critical mass fall in rather than accelerate outward. Such infalling heavy clouds ($M_{\rm crit}\approx0.1$ $M_\odot$ at 1 pc; $M_{\rm crit}$ 10^{-4} $M_\odot$ at 0.3 pc; see Fig. 2) could provide the necessary accreting mass needed to power the QSO. Note also that at the sonic point ($\sim10^{18}$ cm) the critical mass for clouds with densities of 3×10^9 corresponds to column densities of 10^{24} cm^{-2}, about one or two orders of magnitude larger than the observationally inferred values of the BELR clouds. Our model suggests that clouds with column densities $\gg10^{23}$ cm^{-2}

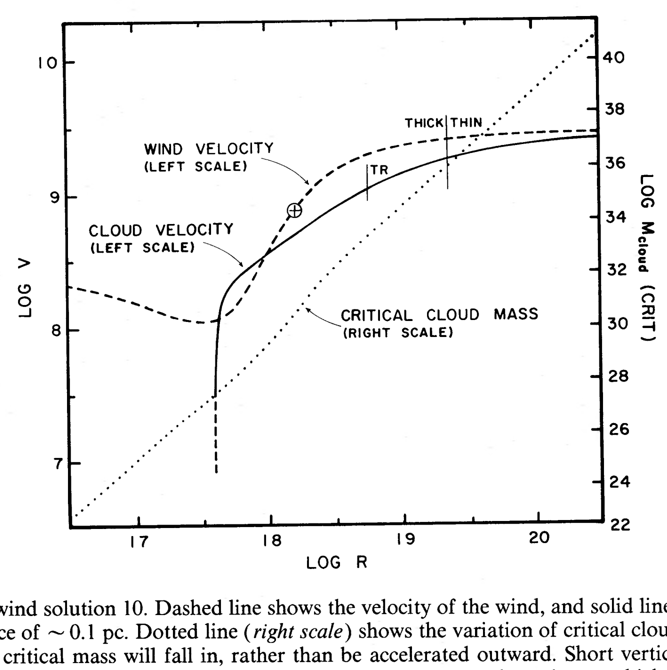

FIG. 2.—Cloud trajectory for wind solution 10. Dashed line shows the velocity of the wind, and solid line shows the velocity of a 2×10^{25} g cloud injected at rest at a distance of ~0.1 pc. Dotted line (*right scale*) shows the variation of critical cloud mass with distance. At a given distance, clouds heavier than this critical mass will fall in, rather than be accelerated outward. Short vertical line marked "TR" shows the point where the clouds were assumed to evaporate to produce the profiles of Fig. 3. The point at which the clouds pass from becoming optically thick to optically thin is also indicated.

are quickly removed from the BELR because of gravitational infall.

As the clouds are accelerated, they are subject to a variety of processes tending to disrupt them. In particular, they will suffer evaporation from the heat conduction associated with the hot thermal gas, and they will suffer ablation of material associated with Rayleigh-Taylor instability. The stability of a fluid mass confined by a combination of ram pressure and gas pressure against disruption by ablation, or more catastrophic disruption by large amplitude Rayleigh Taylor instability, is discussed at length in Paper II. The result is that for clouds suffering instability on their leading edge (i.e., clouds being accelerated up to the wind speed), the characteristic time for ablation is estimated to be comparable to or slightly longer than the acceleration time. For clouds which are still accelerating but moving faster than the wind, the leading edge is Rayleigh Taylor stable (although Kelvin-Helmholtz unstable), and only the trailing edge is Rayleigh Taylor unstable. Under these circumstances the ablation rate is sharply reduced. In neither case does it appear that catastrophic disruption by Rayleigh Taylor instability occurs. Although the momentum flux of the wind is much larger than the radiative momentum flux, we caution that no account has been taken of the effects of the photons on cloud stability.

Destruction of clouds by evaporation associated with thermal conduction has been discussed by Balbus and McKee (1981). Whether or not the clouds can survive for a crossing time depends critically on the strength and topology of the magnetic field. Lacking any knowledge of these parameters, we simply assume the field is such as to prevent immediate evaporation but vary the distance the clouds travel before they dissipate to see how the emission line profiles are affected.

b) Emission Line Profiles

To illustrate the type of emission line profile resulting from the cloud trajectories just discussed, we suppose that a very large number of "standard clouds" are introduced at rest at a distance ~ 0.1 pc (i.e., at about the point of minimum wind velocity). As shown in Figure 2, they rapidly accelerate and are driven past the wind speed by radiation pressure. Because of the rapid acceleration, few clouds are found having $V_{\rm cl} < V_{\rm wind}$ near the injection point, and we ignore the contribution these clouds make to the line profile.

Ignoring the intrinsic line width of each cloud, the flux at a point in the profile with speed y is

$$F(y) = \sum_k \int_{r_k^{\min}}^{r_k^{\max}} \frac{e^{-\tau(r, y/V_{\rm cl})} \xi(y/V_{\rm cl}) E(r) r^2\, dr}{V_{\rm cl}(r)} . \qquad (15)$$

The sum is over those regions $r_{\min} < r < r_{\max}$ for which $V_{\rm cl}(r)$ is greater than y, with y being taken as positive for blueshifted radiation. The clouds will not, in general, radiate line emission isotropically, but will instead radiate according to some function $\xi(\mu)$, where μ is the cosine of the angle between the radius vector and the line of sight. The radiation will also suffer extinction due to scattering (in our case by electron scattering in the thermal wind) by an amount $\exp[-\tau(r, \mu)]$, where τ is the optical depth to the point (r, μ) in the wind. For optically thin lines emitted within clouds containing insignificant amounts of dust, $\xi \equiv 1$. For optically very thick lines (e.g., Lyα) or for lines emitted in a cloud whose rear portions contain substantial amounts of dust, the photons will preferentially diffuse out of the surface of the cloud facing the ionizing source. Hence, ξ will be very small for $\mu = +1$ and largest for $\mu = -1$. We illustrate with the simple function $\xi(\mu) = 1/2(1-\mu)$.

The function $E(r)$ in equation (15) represents the emissivity per unit volume. If clouds are neither created nor destroyed between the assumed injection point and some outer radius where they dissipate, then in this interval the space density of clouds obeys the equation of continuity. In calculating the emissivity of each individual cloud, we have ignored variations in the fraction of the UV radiation going into various lines as the ionization parameter changes and have simply assumed the flux emitted in any line to be proportional to Ωf, where Ω is the solid angle subtended by the cloud to the assumed point source of UV continuum radiation and f is, as in equation (12), the fraction of the incident flux absorbed in the cloud.

The variation with distance of the size of the cloud, its velocity, and f is obtained for a given model by solving equations (12)–(14). Equation (15) is then used to compute the emission line profile. In order to minimize the volume of parameter space within which line profiles were investigated, we constrained the wind solutions by adopting $M = 10^8\ M_\odot$, imposed as before the requirements that $(nT)_{\rm sonic} = 10^{14}$, but also added the requirements that the terminal velocity be 3×10^4 km s^{-1} and the total kinetic energy in the wind at large distances be 10^{46} ergs s^{-1}. These latter two parameters are typical of those required to explain the acceleration of the broad absorption line clouds and the associated absorption line profiles as explained in Paper II. We further arbitrarily assume that the clouds all have a mass of 2×10^{25} g, and are all injected into the flow at the radius where the wind velocity is at its minimum. The wind solution is then characterized by a single free parameter, and the line profiles are characterized by this parameter and by a second parameter, namely, the radius at which the clouds dissipate. Solution (10) of Table 1 is one of these constrained wind solutions which yields a profile in reasonably good agreement with an observed profile.

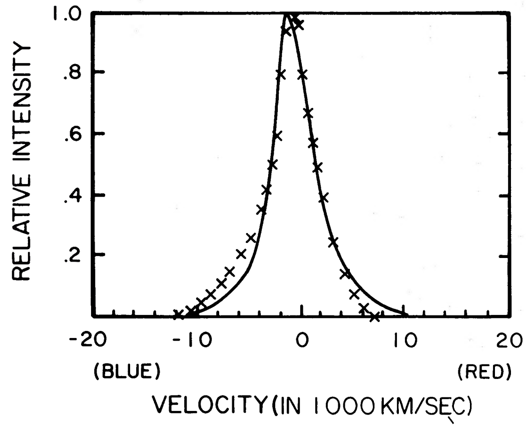

FIG. 3

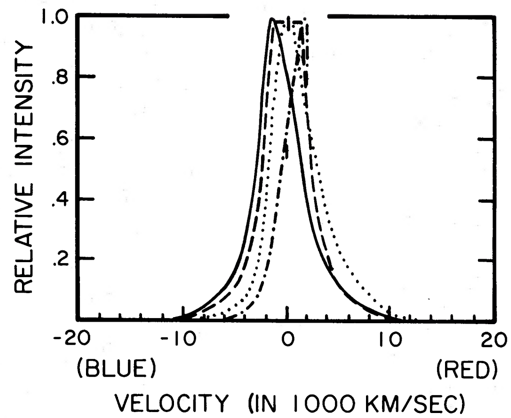

FIG. 4

FIG. 3.—Comparison between an observed profile—Lyα of Q1101-264 (shown with X's)—and a calculated profile based upon wind solution 10 (*solid line*). The calculated profile includes the extinction by electron scattering in the thermal wind, and assumes that the clouds radiate isotropically and dissipate at a distance of ~ 6 pc from the source. The observed line profile has been displaced to the blue by 500 km s^{-1} with respect to the mean quoted redshift of Q1101-264.

FIG. 4.—Effects of electron scattering extinction and angular dependence of the cloud emissivity on the calculated line profiles for wind solution 10. Solid curve, as in Fig. 3, is for the case of electron scattering extinction and isotropic emission. Dashed curve is for no scattering and isotropic emission. (The flat top is an artifact of our cloud injection assumptions). Dash-dot curve is for the anisotropic emission function described in the text with no electron scattering extinction, and dotted curve is for anisotropic emission with electron scattering extinction. Note that all the profiles have arbitrarily been normalized to 1.0 at their peak; this causes artificial differences in the wings. In all cases the clouds were assumed to dissipate at 6 pc.

c) *Discussion of Emission Line Profiles*

In Figure 3 we compare the calculated line profile associated with solution 10 with an observed line profile. The observed profile is the Lyα line (with NV removed) of the QSO 1101-264.[1] The computed profile of Figure 3 includes the effects of electron scattering opacity associated with the wind and is for an isotropic emission function. The peak of the calculated profile is displaced by ~ 500 km s^{-1} to the blue of the QSO rest frame. This profile was calculated with a cloud "dissipation radius" of 2 pc—about 12 times the injection radius. In Figure 4 we show the same theoretical profile with the addition of the profiles for an isotropic emission function without electron scattering and for the "back scatter" emission function, with and without electron scattering extinction. In Figure 5 we also illustrate the growth in the wings if the clouds are assumed not to dissipate until much larger distances.

From these figures we draw the following conclusions: (*a*) it is evidently possible to find parameters for which optically thick clouds, accelerated by the combined effects of the thermal wind and radiation pressure, yield emission line profiles matching observed profiles reasonably well. However, it is by no means true that all of the parameters explored here yield nearly acceptable fits—some of the theoretical profiles are quite grotesque and resemble no observed profiles we know of. (*b*) The fact that observed profiles generally lack the very broad, extended wings shown in Figure 5 suggests that BELR clouds dissipate before they reach their terminal velocity. The lifetime against evaporation would need to be 5 times that estimated by Balbus and McKee. Shields and McKee (1981) noted however, that the low redshift QSO B340 has extended wings in Hα. The observed profile (smoothed by them) is also shown in Figure 5. These authors interpreted these wings as arising from electron-scattered Hα photons in an especially dense

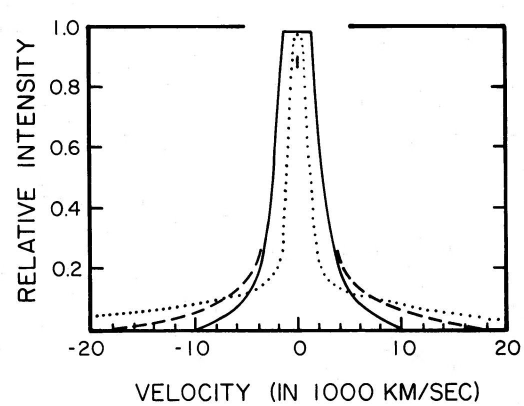

FIG. 5.—Effect of cloud survival on the emission line profiles. Solid curve is for no electron scattering and isotropic emission and cloud dissipation at 6 pc. Dashed curve is identical, except that the clouds are not assumed to dissipate until 200 pc. Dotted line is the (*smoothed*) observed profile for B340, from Shields and McKee (1981).

[1]We thank B. Wilkes and R. F. Carswell for permission to reproduce their profile in advance of publication.

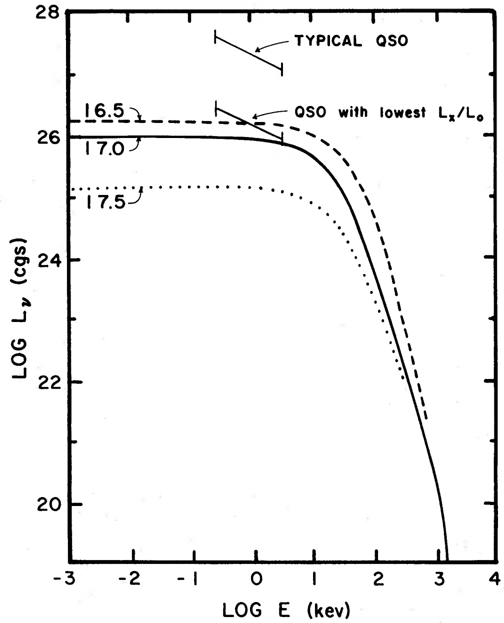

FIG. 6.—Expected X-ray bremsstrahlung spectrum produced by a typical QSO wind. The three curves show how the expected X-ray flux increases as one considers successively smaller values of log R(min), where R(min) is the radius inside which the wind is assumed not to exist. The two short lines represent *observed* monochromatic luminosities (inferred from broad-band measures) scaled to optical luminosities of 10^{46} erg s^{-1} for the case of a typical optically selected QSO and for the QSO with lowest known L_x/L_o.

and cool (10^7 K) confining medium. As noted by these authors, however, the drag associated with such a cool medium would be even more severe than discussed in § II. We suggest instead that especially long-lived clouds like those giving rise to the wings in Figure 5 may be responsible. (The gas in our wind is so hot that the scattered photons are redistributed over too broad a wavelength region to be readily detected). (c) The combined effects of the anisotropic emission for optically thick lines and extinction from electron scattering leave the core of the line virtually unshifted with respect to the QSO rest frame, but it is a prediction of the model that the cores of isotropically radiating lines (e.g., C III] and C IV) should be blueshifted with respect to the QSO rest frame by several hundred km s^{-1}.

Electron scattering by the gas in the wind mainly affects the core of lines, so that the theoretical line profiles for very optically thick lines like Lyα have substantially more emission in the red wing than in the blue wing. In fact, the observed Lyα profiles appear to be generally quite symmetric (Wilkes and Carswell 1981). Several authors have argued that this rules out steady radial flow and have argued for rotation or "turbulent motions" instead. However, the asymmetry which occasionally appears in C IV as extended *blue* emission is very hard to explain without a radial component to the motion.

In addition to the effects of electron scattering and anisotropic emission discussed above, we expect that material ablated off the main clouds will contribute optically thin material radiating isotropically, but it is not clear whether one can add enough of such material to produce symmetrical Lyα wings without producing unacceptable Lyα/Mg II ratios (see also the discussion by Mathews 1981 in this regard).

V. SUMMARY AND DISCUSSION

In the previous sections we have given reasons for thinking that thermal winds driven by relativistic particle heating must be a general feature of QSOs, explored the properties of such winds, and discussed the emission line profiles produced by clouds embedded in them. In this section we consider some additional points of contact between theory and observation, discuss some theoretical problems raised by the model (in particular, the question of Compton losses suffered by the relativistic particles), and indicate some areas where additional observational and theoretical work is required.

a) Additional Observational Constraints

In addition to the line profiles, there are several other observational implications of the wind models. First, inspection of rows 3 and 9 of Table 1 shows that the ratio of $L_{\text{X-ray}}/L_{\text{rel}}$ for all the well-behaved solutions is in the range 1%–10%, with 3% being typical, although this fraction depends upon our choice of an inner radius of 0.03 pc where the integrations were terminated. Since the temperature of the gas is generally $>10^8$ K, most of the energy is emitted above ~ 10 keV. Figure 6 shows the free-free spectrum resulting from the flow of solution number 1, which is typical.

We show for comparison the observed X-ray spectrum of a typical optically selected high redshift QSO. This flux is calculated assuming the X-ray flux is isotropic. Also shown is the X-ray flux for the QSO PG 1351+64 which has the smallest value of L_x/L_o (X-ray to optical luminosity) in the tabulation of Zamorani *et al.* (1981). Since the observations involve broad-band measurements, we convert them to monochromatic fluxes by assuming, following Zamorani *et al.*, that the flux in the region 0.3–3.5 keV has a spectral index of -0.5. We then compare these monochromatic *fluxes* with our own theoretical *luminosities* by scaling the observed optical and X-ray emission to an optical luminosity of 10^{46} ergs s^{-1}. Evidently, the free-free emission makes a significant, but not dominant, contribution to the typical QSO and the dominant contribution to QSOs with very small values of L_x/L_o. Our models predict that values of L_x/L_o lower than ~ 3 times that represented by PG 1351+64 should not occur.

The electron scattering optical depth along a line of sight passing close to the central source significantly affects the core of the emission line profile, as discussed in § IV. The optical depth for the central ray reaches unity for values of $r \approx 0.1$ pc. As noted by Krolik, McKee, and Tarter (1981), this implies that no fluctuations of significant amplitude at any wavelength should occur for QSOs on time scales $\lesssim 1$ month. As far as we are aware, this is true for all radio-quiet QSOs and most radio-selected QSOs but is certainly not true for the compact "OVV" subclass of QSOs. The OVV QSOs we interpret as a phenomenon associated with objects where the jet is sufficiently intense and the orientation such that the thermal gas is swept clear of the axis of the jet which lies approximately along our line of sight.

Since a basic assumption of our model is that a strong flux of relativistic electrons is a universal feature of QSOs, the question arises as to whether our models would predict that *all* QSOs should be observable radio sources. At distances well beyond the BELR, much of the energy of the electrons has been dissipated via the heating mechanism, but within the BELR one might well expect observable radio emission. It is easy to check from our wind solutions that the free-free opacity associated with the wind is much too small to absorb the radio emission. If the magnetic field is not too strong, however, the synchrotron emission associated with the spherical flow of the relativistic particles will not be observed. If we assume a roughly uniform field out to a few parsecs, then the density of $\gamma = 10^3$ electrons in our models implies that this field must be weaker than 10^{-4} gauss in order for the synchrotron radiation from a QSO at $Z \approx 1$ to be < 10 mJ at 6 cm. There are some QSOs which apparently do have a roughly spherical, very compact (< 10 pc) component of radio emission in addition to jetlike structure. We would ascribe this component to an enhanced field strength and/or enhanced diffusion from the site of the relativistic particle production, which we assume is closely connected to the jet.

b) *Potential Theoretical Difficulties*

One difficulty which wind models may encounter involves the rate of mass loss of thermal gas, which, as shown in row 10 of Table 1, is typically 20–30 $M_\odot$ yr^{-1}. This is apparently higher than is readily explainable in terms of deposition of material on an accretion disk by tidal disruption of stars (e.g., Shields and Wheeler 1978), but a mass loss rate of this order follows from *any* dynamical model with pressure-confined clouds embedded in a hot wind. Most of the material in our winds does not, of course, end up on an accretion disk, but can be deposited anywhere within the vicinity of the sonic point. Moreover, there are other mechanisms for removing material from the stars, including ablation by the wind itself, which may make a major contribution to the injection of the thermal gas.

A much more serious problem, in our view, concerns the well-known difficulty of Compton losses by the relativistic electrons. Suppose a particular constituent of the QSO radiation field having luminosity $L_{\rm phot}$ is generated in a shell with radius $R_{\rm iso}$, so that within this distance the radiation field is roughly isotropic. Then, even for radially streaming electrons produced within this region with initial energy $\gamma_{\rm o}$, the distance the electron can travel, $r_{\rm loss}$, before losing a fraction F of its initial energy is

$$r_{\rm loss} \approx \frac{F}{1-F}\frac{m_e c^2}{4/3\sigma_{\rm th} U \gamma_{\rm o}} \approx \frac{F}{1-F}\frac{4\pi R_{\rm iso}^2 m_e c^3}{4/3\sigma_{\rm th}\gamma_{\rm o} L_{\rm phot}}, \quad (16)$$

or

$$(r_{\rm loss})_{\rm pc} \approx 0.1\frac{F}{1-F}\frac{[R_{\rm iso\,(pc)}]^2}{(\gamma_{\rm o})_3 L_{46}^{\rm phot}}, \quad (17)$$

In order to have $r_{\rm loss} > R_{\rm iso}$, we require

$$(R_{\rm iso})_{\rm pc} > 10(\gamma_{\rm o})_3 L_{46}^{\rm phot}\left(\frac{F}{1-F}\right). \quad (18)$$

A criterion which is often invoked in discussions of Compton losses is the condition that the Compton-scattered luminosity not exceed the "seed photon" luminosity. This requires (Jones 1979) that the optical depth of the relativistic electrons to electron scattering multiplied by the energy gain per scattering be less than one; i.e.,

$$\frac{L_{\rm comp}}{L_{\rm seed}} \approx n_{\rm rel}\sigma_{\rm th} R \gamma^2 < 1, \quad (19)$$

where $n_{\rm rel}$ is the characteristic density of relativistic electrons distributed over a region of size R through which the photons must pass to escape. Although equation (19) can be recast in the same form as equation (18) for streaming electrons, the two conditions are not equivalent, and there is no *a priori* reason why equation (19) must be obeyed. In fact, Jones (1979) suggests on the basis of a comparison of the synchrotron, X-ray, and γ-ray fluxes in 3C 273 that equation (19) is violated by a factor of 6.

In order for our models to be consistent, we require that a flux of relativistic particles with luminosity comparable to the photon luminosity be able to survive Compton losses from well within the sonic point (say ~ 0.1 pc) to well beyond the sonic point (say ~ 3 pc). Equation (17) then implies that unless $R_{\rm iso} > 5$–6 pc (as it might be for some component of the radio photons or IR photons generated by dust) the electrons must be continually reaccelerated. (Since it is the electron's γ in the general vicinity of the sonic point that is important in our model rather than some initial γ_0 at some very much smaller radius, starting with a high initial γ_0 is of no help since, for $F \ll 1$, $[1-F]\gamma_0$ is fixed at 10^3, and this determines $r_{\rm loss}$.)

Continual reacceleration would be a serious drain on the source of energy driving the wind. More importantly, however, maintenance of $\gamma = 10^3$ electrons by continual reacceleration would imply Compton luminosities substantially in excess of $L_{\rm rel} \approx 10^{46}$ ergs s^{-1} in the X-ray and/or γ-ray region It is therefore important to know, either on theoretical or observational grounds, what constituents of the photon field having $R_{\rm iso} < 5$–6 pc are likely to be present.

There are at least two components to consider. First, in our model, thermal bremsstrahlung is produced throughout a region with $R \sim 0.1$ pc and with L_{46} typically ~ 0.03. This would lead to $r_{\rm loss} \approx 0.03$ pc. In fact, however, most of these photons appear relativistic in the rest frame of a $\gamma = 10^3$ electron, and the Compton losses are strongly reduced (Jones 1965). For example, the loss rate is only 10% of that implied by equation (17) for a photon of 500 eV scattering off $\gamma = 10^3$ electrons, and even at a temperature of 2×10^8 K, only 3% of the photons have energy less than this. The thermal bremsstrahlung associated with the wind does not, therefore, cause a serious Compton problem.

Second, since a typical observed QSO optical luminosity is 10^{46} ergs s^{-1}, if the value of $R_{\rm iso}$ associated with this optical radiation were <1 pc, then (see eq. [17]) $r_{\rm loss}$ would be <0.1 pc, but this is just the size of the region inside the sonic point where the heating from the electrons is required. However, if the electron pitch angle distribution is strongly peaked in the radial direction, the losses caused by a radiation field which is also radially streaming are sharply reduced, as first pointed out by Woltjer (1966). The actual size of the region where either nonthermal or thermal optical photons are generated is, in fact, very likely to be smaller than 1 pc, but electron scattering from the wind, discussed above, ensures that this radiation field *cannot be radially streaming within* ~ 0.1 *pc*. Thus, $r_{\rm loss}$ must be only $\sim 10^{-3}$ pc inside this point. Beyond this point, however, increasing radial streaming of the radiation field causes the Compton losses to drop extremely sharply for electrons whose pitch angles are strongly peaked in the radial direction.

As an illustration of this effect consider a sphere with a radius of 0.1 pc radiating isotropically from its surface at a rate of 10^{46} ergs s^{-1}. Whereas a $\gamma = 10^3$ electron can travel only 10^{-3} pc if placed *inside* the sphere before losing half its energy, such an electron, *traveling radially*, can escape to infinity, with the loss of only one-half its energy, if injected only 0.015 pc above the surface of the sphere.

In order to avoid catastrophic Compton losses, therefore, our wind models require that (a) acceleration mechanisms must exist out to the point where the opacity to electron scattering becomes small (0.1 pc); (b) the relativistic electrons must have their pitch angles strongly peaked in the radial direction. So little is understood about the mechanism for producing relativistic particles in QSOs that we do not know whether requirement (a) is or is not reasonable.

With respect to the question of the electron pitch angle distribution, the Larmour radius of $\gamma = 10^3$ electrons is exceedingly small compared to the scale of the flow, even for magnetic energy densities many orders of magnitude below the equipartition value. It might be supposed, therefore, that the distribution of the momentum vectors of the electrons would not be nearly radial as we require, but would be nearly isotropic. The following arguments suggest this supposition is probably not correct. Even in radio sources, most models suggest $B^2/8\pi < U_{\rm rel}$. If we are correct in our conjecture that radio-quiet QSOs are radio quiet because the fields are small and not because the particles are absent, this inequality is even more strongly obeyed. Under such circumstances the ambient static field is likely to be combed radially over large portions of the flow. Therefore, time-dependent fields in the super-Alfvenic streaming modes excited by the relativistic electrons (see Morrison *et al.* 1981) completely dominate the static field in determining the electron pitch angle distribution. For the ratio of relativistic to thermal particle densities occurring in the wind models, the phase velocity of the waves is mildly relativistic, but the exact phase velocity is difficult to evaluate since the expressions of Morrison *et al.* break down as $V_{\rm phase}$ approaches c. The relativistic particles are quickly trapped by the rapidly growing waves and convected out at the phase velocity of the wave. In the frame moving with the phase velocity of the waves, the pitch angle distribution of particles is likely to be only mildly peaked in the direction of the propagation vector, but in the frame of the QSO it will be strongly peaked, by abberation, in the direction of the propagation vector. However, the propagation vectors themselves are essentially radial, being determined by the direction of the bulk momentum vector of the relativistic electrons.

Inside the electron scattering radius, Compton losses will, in fact, probably prevent the electrons from becoming more than mildly relativistic. Even so, whatever acceleration mechanisms are at work may still strongly heat the gas, although the heating law will no longer be that of equations (5) and (6).

c) *Summary and Suggestions for Further Work*

Thermal winds heated by relativistic electrons are postulated to be characteristic of all QSOs. Models of these winds require acceleration of electrons to occur out to distances of ~ 0.1 pc. The models yield X-ray thermal bremsstrahlung amounting to $\sim 3\%$ of the relativistic particle luminosity. Electron scattering masks variations occurring on time scales $\lesssim$ months. Compton losses occurring in the region where $\tau_{els} < 1$ probably create a photon luminosity in the 10^4–10^8 eV range comparable to the luminosity in the optical and near-IR. The characteristic scale of the BELR, set by the sonic point radius, is slightly less than 1 pc for a wide range of wind parameters. The predicted sonic point radius, and hence size of the emission line region, scales in such a way that the ionization parameter is nearly constant over a wide range of luminosity. The wind model may therefore be applicable to Seyfert nuclei as well as QSOs. Emission line profiles can be produced by the combined effects of the wind and radiative accelerations which match the general features of the observed profiles, but the production and survival of the emission line clouds is not yet understood well enough to make this a critical test. Clouds with column densities more than an order of magnitude larger than the "standard cloud" would fall inward if injected at ~ 0.1 pc, while clouds much smaller than the standard cloud will be selectively destroyed by ablation, evaporation, and other processes discussed by Krolik, McKee, and Tarter (1981). As shown in Paper II, winds having the parameters which adequately account for the observed properties of the BELR are also able to reproduce the observed features of broad absorption lines in QSOs. In Paper II we also present a more general overview of the structure of QSOs from the scale of the BELR ($\sim$ pc) to the much larger scale of the BALR ($\sim$ kpc).

While our model can reproduce the general features of the BELR line profiles, it does not account for the extended emission sometimes seen on the blue wing of C IV and Lyα in high redshift QSOs (Young, Sargent, and Boksenberg 1981; Wilkes and Carswell 1981). It might have been supposed that the electron scattering opacity in the wind would produce precisely such an effect since the line of sight to the material producing the emission with the largest redshift suffers the greatest extinction. However, the region of significant electron scattering is so small compared to the region where the flow has attained its terminal velocity that a line-of-sight passing outside this region still strikes clouds in the high-velocity portion of the BELR in such a way that the cosine of the angle between the line of sight and the velocity of the clouds is still nearly 1.0. In fact, it is the red side of the *core* of the profile produced inside the electron scattering region which is most strongly attenuated. This displaces the *core* to the blue and makes it appear as if the wings in optically thin lines are asymmetric to the red. As noted above, the anisotropic emission of optically *thick* lines, combined with electron scattering, produces cores which are virtually undisplaced.

A related problem is the lack of large consistent substantial differences between the observed profiles of lines expected to be anisotropically emitting (e.g., Lyα) and those expected to be isotropically emitting (C IV, C III]). These two problems are by no means unique to our model, however: The observed blue asymmetry is a severe problem for all models without radial flow, and the lack of a large Lyα/C IV profile difference is a problem for all models with radial flow.

We speculate that dust may condense and survive in the rear of thick clouds where the gas is cooler and shielded from much of the high energy photon flux. If the cloud is optically thick due to dust, then all lines behave to a certain extent as anisotropic emitters. Since the covering factor is small, the continuum would be relatively unaffected. This effect, when combined with the addition of high velocity emission from optically thin cloudlets ablated off the main clouds, will blur the differences between C IV, C III], and Lyα. Some general extinction of the emission from all the receding clouds seems required to explain the extended blue emission. This could arise from dust concentrated in a thin plane which is an extension of the accretion disk.[2] Shielding by the disk itself, together with the small solid angle presented by an edge-on disk, would allow dust to survive as close as ~ 1 pc to the continuum source. The source would create a cavity around the dust, leaving the continuum source unreddened. For further interesting speculation on these problems see the discussion by Mathews (1981) and Wilkes and Carswell (1981).

From the theoretical point of view, development of a fully self-consistent wind model of the BELR in QSOs requires further work in at least three areas: (a) clarification of how matter is injected into the flow, either from stars or boil-off from an accretion disk; (b) development of models concerning the condensation and subsequent disruption of the emitting clouds; (c) identification of the principal mechanism responsible for relativistic particle acceleration and propagation. Even after this has been accomplished, many very complex details must be worked through. Specifically, whatever acceleration mechanism is at work will produce electrons with a spread of γ's. We have argued that particles with $\gamma \ll 10^3$ will quickly lose their energy to the thermal gas (thus injecting a "thermal pulse" into the wind near the base of the flow), while particles with $\gamma \gg 10^3$ will quickly lose their energy in the form of X-rays and γ-rays via the Compton process, leaving particles with $\gamma \approx 10^3$ able to deposit energy over scales comparable to the BELR. In order to quantitatively investigate both these losses a detailed analysis of the evolution of the phase space distribution of the relativistic electrons, taking into account their interactions with the plasma waves, the thermal gas, and the radiation field, as well as with the processes producing the acceleration, must be carried

[2] We thank T. Heckman for this suggestion.

out. This is a very difficult but important problem to attack.

This work was supported by NSF grants AST-8109025 and 7923772 which are gratefully acknowledged. W. A. C. acknowledges assistance from the Morehead Foundation and thanks KPNO and Steward Observatory for their hospitality. We also acknowledge valuable discussions with a number of colleagues, including B. Wilkes, C. McKee, G. Shields, C. Foltz, B. Peterson, and E. Capriotti. We thank E. Capriotti for an inspiring preprint.

After this work was completed we received a preprint by Beltrametti and Drew (1982) on electron scattering and X-ray emission reaching conclusions similar to those reported here.

REFERENCES

Angel, J. R. A., and Stockman, H. S. 1980, *Ann. Rev. Astr. Ap.*, **18**, 321.
Balbus, S. A., and McKee, C. F. 1981, preprint.
Baldwin, J. A., and Netzer, H. 1978, *Ap. J.*, **226**, 1.
Beltrametti, M. 1981, *Ap. J.*, **250**, 18.
Beltrametti, M., and Drew, J. 1982, *Astr. Ap.*, in press.
Bignami, G. F., *et al.* 1981, *Astr. Ap.*, **93**, 71.
Blumenthal, G. R., and Mathews, W. G. 1975, *Ap. J.*, **198**, 517.
______. 1979, *Ap. J.*, **233**, 479.
Capriotti, E., Foltz, C., and Byard, P. 1980, *Ap. J.*, **241**, 903.
______. 1981, *Ap. J.*, **245**, 396.
Carswell, R. F., and Ferland, G. J. 1980, *M.N.R.A.S.*, **191**, 55.
Edwards, A. C. 1980, *M.N.R.A.S.*, **190**, 757.
Eilek, J. A., and Caroff, L. J. 1979, preprint.
Jones, F. C. 1965, *Phys. Rev.*, **137B**, 1306.
Jones, T. W. 1979, *Ap. J.*, **233**, 796.
Jones, T. W., and Hardee, P. E. 1979, *Ap. J.*, **228**, 268.
Krolik, J. H., McKee, C. F., and Tarter, C. B. 1981, *Ap. J.*, **249**, 422.
Kwan, J., and Krolik, J. H. 1981, preprint.
Mathews, W. G. 1981, preprint.
Morrison, P. J., Scott, J. S., Holman, G. D., and Ionson, J. A. 1982, *Ap. J.*, submitted.
Scott, J. S., Christiansen, W. A., Weymann, R. J., and Schiano, A. V. R. 1982, *Ap. J.*, submitted (Paper II).
Scott, J. S., Holman, G. D., Ionson, J. A., and Papadopoulos, K. 1980, *Ap. J.*, **239**, 769.
Shields, G. 1977, *Ap. Letters*, **18**, 119.
______. 1978, in *Pittsburgh Conference on BL Lac Objects*, ed. A. M. Wolfe (Pittsburgh: University of Pittsburgh), p. 257.
Shields, G., and McKee, C. F. 1981, *Ap. J.* (*Letters*), **246**, L57.
Shields, G. A., and Wheeler, J. C. 1978, *Ap. J.*, **222**, 667.
Smith, M. G., *et al.* 1981, *M.N.R.A.S.*, **195**, 437.
Wilkes, B. J., and Carswell, R. F. 1981, preprint.
Woltjer, L. 1966, *Ap. J.*, **146**, 597.
Young, P., Sargent, W. L. W., and Boksenberg, A. 1981, preprint.
Zamorani, G., *et al.* 1981, *Ap. J.*, **245**, 357.

WAYNE A. CHRISTIANSEN, A. V. R. SCHIANO, J. S. SCOTT, and R. J. WEYMANN: Steward Observatory, University of Arizona, Tucson, AZ 85721